The Sixteenth International Symposium on Artificial Life and Robotics 2011 (AROB 16th '11),
B-Con Plaza, Beppu,Oita, Japan, January 27-29, 2011

A Neuro PID control of Power Generation using Low Temperature Gap

Kun-Young Han, Hee-Jae Park, and Hee-Hyol Lee

The Graduate School of Information, Production and Systems, Waseda University, Kitakyusyu, 808-0135, Japan
2-7 Hibikino, Wakamatsu-ku, Kitakyushu, Fukuoka 808-0135, Japan
(Email address: kyhan@akane.waseda.jp)

Abstract: Recently, renewable energy is increasingly attractive in solving global problem such as the environmental pollution and energy shortage. Among varieties of renewable energy resource, power generation using low temperature gap has received much attention of researchers. However, this system is difficult to control because each of the components of this system, such as heat exchanger, working fluid and turbine, has a dynamic characteristic or nonlinear factor. In order to overcome this problem, PID controller based on neural network for power generation using low temperature gap is designed to keep the stable speed of the steam turbine in real environment.

Keywords: Power generation, Evaporator, Turbine, PID control, neural network

I. INTRODUCTION

A strong interest in distributed generations using renewable energy such as wind and solar energy have been attracted because the fossil energy will be exhausted in the future and its use causes the environmental issue. Among them, there is some renewable energy that has not yet been used, such as the heat from hot springs or exhaust heat from factories. However, the power generation using these unused renewable energies can only produce a small amount of heat but also have relatively low heat efficiency. Moreover, these heat sources are scattered and their scale are small[1]. Therefore, the suitable control methods must be developed to overcome these problems in that capacity and scale.

On the other hand, the power generation using the low temperature gap used in this paper includes dynamic characteristics and nonlinear factors. Although this system contains these complex factors, most of the control algorithms are based on linear models. The linear models deduced from step responses and impulse responses are desirable, because they can be identified in a straightforward manner. In addition, a goal for most of the applications is to maintain the system at a desired steady state, so a precisely identified linear model is sufficiently accurate in the neighborhood of an operating point. As this point of view, the power generation using low temperature gap based on the approximate linear models are designed in this paper.

PID control is used in process field in generally. Despite PID controllers are applicable to many controlled system, it performs poorly in complex system. Therefore, PID controller cannot be applied directly in the complex systems. In this paper, an improved neural network, which shows excellent performance for nonlinearity is applied to the power generation using temperature gap. Initial values of a neuro PID controller use the parameters obtained from the linearized model. This paper composed as follows. The power generation system using low temperature gap and each of the components such as an evaporator and a condenser based on heat balance equation, and a turbine element are modeled in Section 2. In the section 3, a traditional PID control is introduced and a neuro PID controller is proposed for the power generation using low temperature.

II. Dynamic modeling of power generation using low temperature gap

The main components of the power system using the low temperature gap with closed cycle are constructed of the heat exchanger (evaporator and condenser), turbine, and pumps. The simple structure of the power generation system using the low temperature gap is shown in Fig.1.

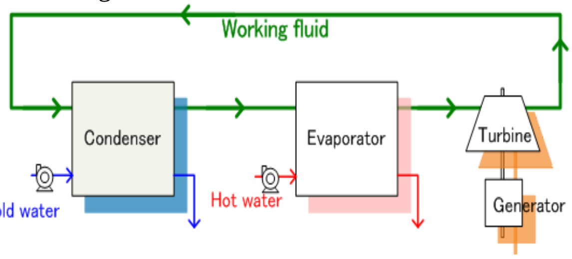

Fig.1. Power generation using the low temperature gap with closed cycle.

2.1 Evaporator model

The evaporator is a shell-and-tube type as shown in Fig.2. The working fluid is a liquid and moves to the evaporator by a pump. And then the working fluid is boiled and changed to steam in the evaporator by hot water.

Modeling assumption

1) Working fluid evaporating pressure is constant in static state.
2) Latent heat of working fluid keeps no change.
3) Evaporating flow supplies a quantity of heat.

The heat balance equation of hot water, the working fluid, and supply heat are defined as follows [2].

$$\upsilon_h(\partial\theta_h/\partial x)+(KU/\omega_h)(\theta_h-\theta_s)=0 \quad (1)$$

$$G_\upsilon(h''-h')=Q \quad (2)$$

$$Q=\int_0^L KU(\theta_h-\theta_s)dx \quad (3)$$

where, υ_h is a speed of a moving fluid of hot water, θ_h is a temperature of hot water, x is a distance, K is a heat transmission coefficient, U is a heating surface area per unit time, ω is heat capacity per unit time and θ_s is a temperature of saturated water vapor .

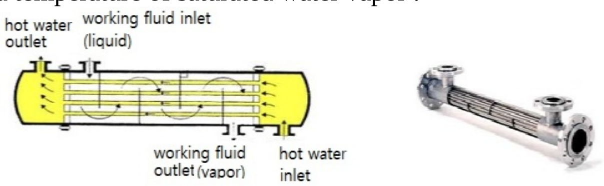

Fig.2. Structure of the evaporator

2.2 Turbine model

The turbine is composed of the steam control valve and a rotor blade. The block diagram of the turbine is shown in Fig.3. The steam is moved from the evaporator to the turbine blade through the steam control valve. It adjusts the flow of steam to the turbine blade. The equations of the turbine systems are given as follows [3]. Mass rate and a control valve of the working fluid steam are defined by Eqs.(4),(5), respectively, and the turbine blade speed is defined by Eq.(6)

$$\mu_T=\frac{\alpha_T\dfrac{A_1}{A_E}}{M_E\left[\upsilon(\alpha_T)\right]^{1/2}}\left(P_E-P_T\right)^{1/2} \quad (4)$$

$$a_1\frac{dx_1}{dt}=K_3\left(\frac{\upsilon}{\upsilon_{\max}}\right),\ \ (0\le x_1\le 1) \quad (5)$$

$$\frac{d\upsilon}{dt}=\frac{1}{\tau_T}\left[\frac{P_E'-P_T'}{\overline{P_E'}-\overline{P_T'}}\frac{\mu_T}{\upsilon\overline{\mu_T}}-(1-\eta)\frac{\xi(t)}{\upsilon}-\eta\upsilon^2\right] \quad (6)$$

where, α_T is a area of divergence of the valve, A_1/A_E is a cross-sectional area of a pipe leading from the evaporator to the turbine, P_E is a vapor pressure at the evaporator outlet, P_T is a vapor pressure at the turbine outlet, K_3 and a_1 are the gain, $v_{\max}$ is a maximum speed of the turbine blade, M_E is a constant parameter, τ_T is a system constant, η is a coefficient of loss, ξ is a electric load, and $\overline{P_E'}$, $\overline{P_T'}$, $\overline{\mu_T}$ are desire values.

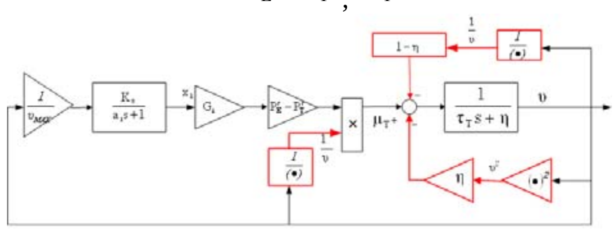

Fig.3. Block diagram of turbine

Linear approximate turbine model

The linear approximate turbine model is obtained by approximating the turbine. Fig.4 shows the linear approximate turbine model, which includes 1st and 2nd order delay elements and dead time element.

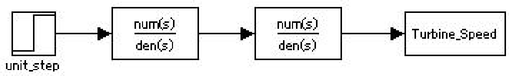

Fig.4. Linear approximate turbine model

2.3 Modeling of power generation system as MIMO system

The evaporator and the condenser are modeled as a multi-input multi-output model(MIMO) illustrated in Fig.5.

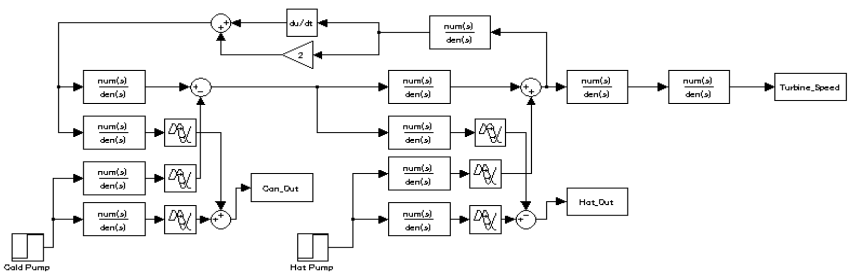

Fig.5. MIMO system for the Power generation

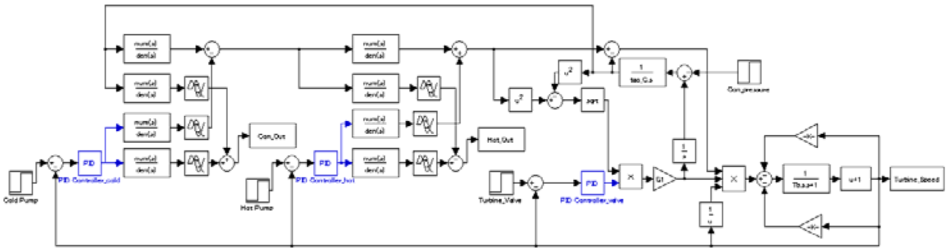

Fig.7. Block diagram of Power generation system with PID controller

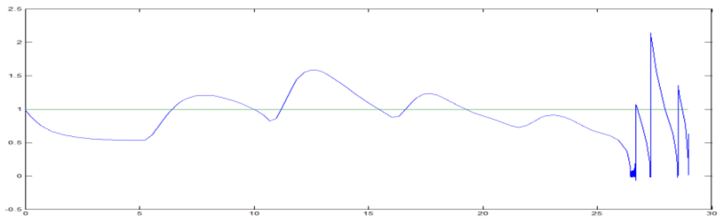

Fig.8. Result of control using PID controller

III. Neuro PID controller

3.1 PID Control

A schematic of a system with a PID controller is shown in Fig.6. The PID controller compares a measured process value y with a reference value r. The difference or error e is then processed to calculate a new process input u. This input will try to adjust the measured process value to the desired value. PID controller is widely used in industrial control systems.

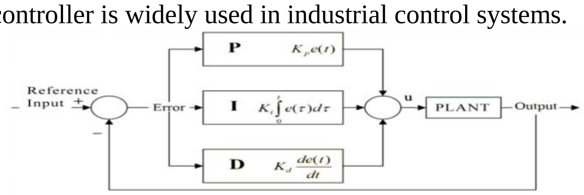

Fig.6. Block diagram of a PID controller

PID algorithm is formed as follow,

$$u(t) = K_p e(t) + K_i \int_0^t e(\tau)d\tau + K_d \frac{d}{dt} e(t) \qquad (7)$$

where, K_p is proportional gain, K_i is integral gain, K_d is the differential gain, and $e(t)$ is the error.

3.2 PID tuning

There are several methods for tuning the PID parameters. The parameters are obtained by using the step response method and the ultimate sensitivity method. Fig.7 represents the block diagram of the power generation system with PID controller, and Fig.8 is a result of control using PID control.

3.3 Neuro PID Controller

The PID controller does not lead to good performance. In this paper, PID controller with a neural network is considered, and shown in Fig.9.

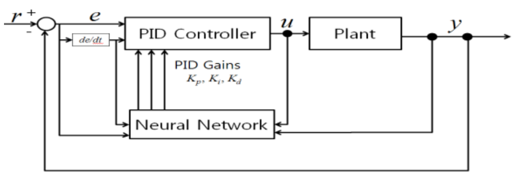

Fig.9. Structure of neuro PID controller

BP network structure

The BP neural network is a multi-layer perception neural network, which consists of three components: input layer, hidden layer, and output layer. The output layer corresponds to the values, which are three adjustable parameters K_p, K_i, *and* K_d, as shown Fig.9. Therefore, each of parameters can be adjusted by self learning ability of the neural network. And the best values of them can be obtained corresponding to the outputs of BPNN with a certain optimal control law. The PID algorithm is given by Eq.(8).

$$\begin{aligned} & u(t) = u(t-1) + \Delta u(t) \\ & \Delta u(t) = u(t-1) + K_p(t)(e(t) - e(t-1)) + K_i(t)e(t) \\ & \qquad + K_d(t)(e(t) - 2e(t-1) + e(t-2)) \\ & e(t) = r(t) - y(t) \end{aligned} \qquad (8)$$

where, u is the control value, r is the reference value, and y is the actual output value. On the other hands, the inputs and outputs of the hidden layer in the neural network are given by Eq.(9).

$$\begin{aligned} & net_i^2(t) = \sum_{j=0}^{M} w_{ij}^{(2)} O_j^{(1)} \\ & O_i^{(2)}(t) = f(net_i^2(t)) \quad (i = 1,2,\cdots,Q) \\ & net_l^{(3)}(t) = \sum_{l}^{Q} w_{li}^{(3)} O_i^{(2)}(t) \\ & O_l^{(3)}(t) = g(net_i^3(t)) \quad (l = 1,2,3) \end{aligned} \qquad (9)$$

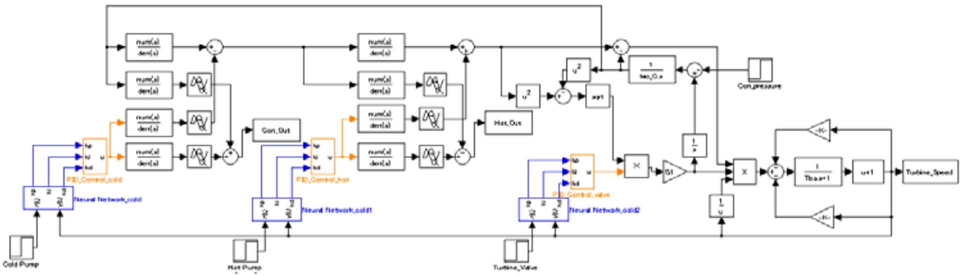

Fig.10. Block diagram of Power generation system with Neuro PID controller

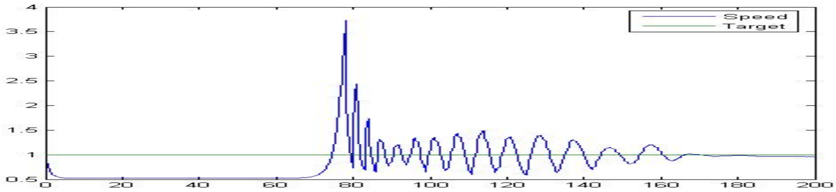

Fig.11. Result of control using Neuro PID controller

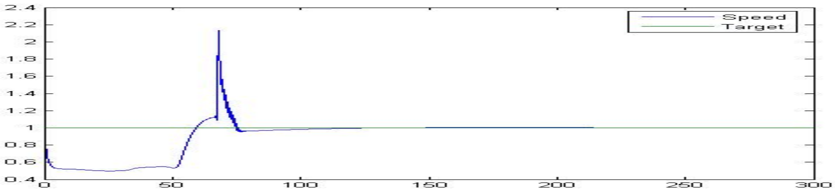

Fig.12. Result of control of Neuro controller using the initial value based on linearized model

where, M and Q are the neuron numbers of the input and hidden layer, respectively, w is the weight, net is the input, and O is the output. The superscript (1), (2) and (3) denote the input, the hidden, and the output layer. f and g are activation functions of the hidden layer and the output layer. Obviously, $O^{(3)}$ is K_p, K_i and K_d. Parameters of K_p, K_i and K_d, which are obtained from the linear approximate model, are used as initial values in this paper. The weights of BPNN are updated according to the gradient-descent algorithm.

$$\Delta w(t) = -\eta[\partial E(t)/\partial w(t)] + \alpha \Delta w(t-1) \qquad (10)$$

where, η and α are defined as learning rate and inertia factor, respectively. The inertial item $\alpha \Delta w(t-1)$ is added to accelerate convergence. The manual differentiation method is used to increase the accuracy the value of $\partial E(t)/\partial w(t)$ in Eq.(10). The algorithm of updating the weights for the output layer is given as follows.

$$\Delta w_{li}^{(3)}(t) = \alpha \Delta w_{li}^{(3)}(t-1) + \eta \delta_l^{(3)} O_i^{(2)}(t)$$

$$\delta_l^{(3)} = e(t)\,\mathrm{sgn}\left(\frac{\partial y(t)}{\partial \Delta u(t)}\right) \frac{\partial u(t)}{\partial O_l^3} \dot{g}(net_l^{(3)}(t)) \quad (l = 1,2,3) \qquad (11)$$

The process to acquire $\partial E(t)/\partial w(t)$ is complex and fallible especially when the activation functions are complicated or Q is greater than 1. Besides that, according to Eq.(11), the value of the item $\partial y(t)/\partial u(t)$ is substituted by its sign function. That is to say, it is set to be 1 or -1. The impreciseness produced here can be compensated by η. The PID controller with BPNN is applied as shown in Fig.10, and a result of PID control using BPNN is represented in Fig.11 while K_p, K_i, K_d do not use as initial value. A result of PID control using BPNN is shown in Fig 12 while the initial values of K_p, K_i, and K_d are used based on the linearized model.

V. Conclusion

The power generation system, which consists of the evaporator, the condenser, and the turbine are designed. The conventional PID controller has the advantage of simple structure, good stability, easy to engineering implementation and so on. However, for the complex system such as the power generation system using low temperature gap using the traditional PID control is more difficult to obtain good control performance. This paper combines the BP neural network and PID control. The PID parameters from the linear model are used as initial value in the output layer of BPNN. The neuro controller proposed is successfully implemented.

REFERENCES

[1] Satomi S, K-Y H, J-S S, et.al (2010) A learning control of unused energy power generation. International symposium on AROB 15th.
[2] Hashizume T, Kawai S, Machiyama T (1981) Experimental studies on the dynamic characteristics of evaporator in the L.B.M. turbine system. Jpn Soc Mech Eng C 47(421):1161–1168.
[3] Owens WL (1982) OTEC plant response and control analysis. ASME J Solar Energy Eng 104:208–215.